# Label-free detection of C-Reactive protein using bioresponsive hydrogel-based surface relief diffraction gratings

María Isabel Lucío,[a,1] Andy Hernández Montoto,[a,1] Estrella Fernández,[a] Sabri Alamri,[b] Tim Kunze,[b] María-José Bañuls,[a,c,*] Ángel Maquieira[a,c]

[a]Instituto Interuniversitario de Investigación de Reconocimiento Molecular y Desarrollo Tecnológico (IDM), Universitat Politècnica de València, Universitat de València, Camino de Vera s/n, 46022 Valencia, Spain.

[b]Fraunhofer-Institut für Werkstoff- und Strahltechnik IWS, Winterbergstr. 28, 01277 Dresden, Germany.

[c]Departamento de Química, Universitat Politècnica de València, Camino de Vera s/n, 46022 Valencia, Spain.

[1]These authors contributed equally to this work.

*Corresponding author email: mbpolo@upv.es

## Highlights

- A novel label-free biosensing system based on surface relief gratings fabricated with responsive hydrogels has been developed for determination of CRP.
- Label-free sensing of CRP at a suitable concentration range for clinical applications was achieved using a homemade measurement setup.
- Amplification strategies were applied which improved the analytical performance of the sensor.

- The approach was successfully applied to determine CRP in certified human serum sample sensitively and specifically.

**Abstract**

Responsive hydrogel-based surface relief gratings have demonstrated great performances as transducers in optical sensing. However, novel and smart designs of hydrogels are needed for the appropriate detection of analytes and biomolecules since the existing materials are very limited to specific molecules. In this work, a biosensing system based on surface relief gratings made of bioresponsive hydrogels has been developed. In particular, the hydrogel contains phosphocholine moieties to specifically recognize C-Reactive protein (CRP). The CRP-Sensing hydrogel capacity to selectively detect CRP was fully demonstrated. Using Direct Laser Interference Patterning, micro-gratings were created on CRP-Sensing hydrogel substrates and applied for the label-free sensing of CRP using a simple laser-based homemade optical setup. Limits of detection (LOD) and quantification (LOQ) in human serum dilutions of 1.07 and 8.92 mg $L^{-1}$, respectively, were reached. These results demonstrate that the biosensing system allows the selective label-free detection of CRP within concentration ranges around those related to risks of cardiovascular diseases and sepsis. Besides, amplification strategies have been carried out improving the sensitivity, widening the linear range, and reaching better LOD and LOQ (0.30 mg $L^{-1}$ and 4.36 mg $L^{-1}$). Finally, all the approaches were tested for the quantification of CRP in certified human serum with recoveries of around 100%.

**Keywords** Biosensor; diffraction; label-free; surface relief gratings; responsive hydrogel, C-Reactive protein

## 1. Introduction

Diffraction gratings are interesting implements as transducers for the label-free sensing of specific molecules. When a collimated beam illuminates the grating, this generates a diffraction pattern in which the diffraction order intensities and/or positions depend on the geometrical and optical characteristics of the grating. If these properties are modified, a change in the produced signal is observed (*i.e.* the diffraction pattern). The modifications in the grating can be generated by physical stimuli (for example, pressure, temperature, etc.) or by the interaction with an analyte, thus the grating becomes a specific sensor for this specific analyte. Gratings of proteins immobilized on solid surfaces (biogratings) have been applied with great success for the label-free detection of biomolecules[1–3] and low molecular weight organic compounds.[4] In addition, biogratings have been also implemented in optical fibers to sense biorecognition events by some of us, which constitutes a new promising transduction system.[5] In these approaches, the amount of matter that constitutes the grating changes after the biorecognition event and this results in a modification of its diffractive performance. These biosensing systems are considered simple, inexpensive, and very efficient when compared with other label-free sensing systems. One way to fabricate biogratings is using a master grating and replicate this on a substrate, either for microcontact printing biomolecules[6] or for molding a biomaterial.[7] Master gratings can be produced by means of several techniques and a simple, yet effective, method is using laser surface texturing (LST). In fact, guiding a focused laser beam on a substrate, a large variety of materials like metals, ceramics, and polymers can be processed creating a large number of possible periodic textures.[8,9] Despite the easy processing, regular periodic features with lateral dimension smaller than 10 µm are not easily achievable with conventional LST approaches, which strongly limits the detection of a diffraction pattern. A well-established laser technique able to produce

periodic structures in the micro- and sub-micrometer range is Direct Laser Interference Patterning (DLIP). This method relies on the overlap of two or more coherent laser beams, where an interference pattern is locally created on a surface. At the intensity maxima positions, the material is directly ablated, while at the minima, it remains unaffected, creating structures much smaller than the beam size itself.[10,11] In particular, DLIP has been employed to treat several materials like metals or polymers for the fabrication of regular 1D and 2D periodic structures which act as diffraction gratings for decoration and product protection.[12–14]

Hydrogels are 3D polymeric networks that can absorb high quantities of water without collapsing. They have a porous structure that allows the diffusion of molecules within their matrix and they can be smartly designed to respond to external stimuli (responsive hydrogels).[15] This response is normally due to a macroscopic change, usually a volume change, that occurs after the interaction of the polymer chains with the stimuli. The stimuli can be physical (e.g. temperature, electric and magnetic field, mechanical stress) or chemical (pH and chemical molecules). Particular hydrogels (bioresponsive hydrogels) are designed to respond even to a specific biorecognition event.[16] Hydrogels have been used as active transducers in optical systems based on photonic crystals,[17–19] holography[20–24], microlenses,[25] or optical fibers[26–28] for glucose detection. Wang et *al.* introduced for the first time their use for the fabrication of surface relief diffraction gratings.[29] They produced three dimensional periodic structures on the hydrogel surface that structurally changed upon interaction with glucose. These structural changes resulted in a modification of the intensity of the diffracted light by the grating, and so the diffraction efficiency, which could be monitored upon the addition of increasing glucose concentrations. The same principle has been used for the sensing of heavy metals,[30] pH,[31] and ethanol.[32] In terms of biosensing, hydrogel gratings have been scarcely reported, and

few examples are found where they are used for the detection of Thrombin[7] and Human Immunoglobulin-G.[33,34] These systems make use of displacement assays within the hydrogel matrix to produce the volumetric changes that generate the analytical signal, and, although the principle is nicely demonstrated, there is still room for improvement. Firstly, using a target direct biorecognition rather than a displacement reaction is always preferable, as direct assays are simpler, faster, and less error-prone; secondly, up to our knowledge, no measurements in real matrices, such as blood serum, have been still demonstrated; and thirdly, only sensitivities in the mg $mL^{-1}$ range have been reported, which is larger than the regular concentration of most analytes of interest. In brief, new appropriate smart designs of hydrogels should be carried out to open the door to the detection of new and much more analytes.

The different disorders that affect heart and blood vessels are grouped as cardiovascular disease (CVD). CVD causes more than 17.9 million deceases over the world each year, which stands it as the main cause of death globally.[35] Among different biomarkers, Human C-Reactive protein (CRP) is a well-known analyte for prognosis of cardiovascular risk and, in addition, it can offer information about patients suffering sepsis and inflammatory processes,[36] illnesses that also deserve a short response time in hospitals.[37] Immunoassays are the most utilized methods for the determination of C-Reactive protein nowadays,[38] but biomimetic alternative methods are emerging.[39–41] These methodologies use phosphocholine derivatives as sensing probes since it is a natural receptor of CRP present in bacterial cell wall;[42] besides, phosphocholine has excellent antifouling properties that can block unspecific interactions. The easy recognition of CRP by the phosphocholine units has been previously utilised to develop hydrogels for the successful fluorometric detection of CRP in microarray format.[43] The hydrogel platform was also used for immunoassays and oligonucleotide hybridization assays as well as for the

interferometric label-free detection of CRP in blood serum using the Biophotonic Sensing Cell named BICELLs, however this transducer requires micro/nano fabrication facilities, and a special optical measurement platform.[43]

Based on previous work, here we aim to demonstrate the potential of the approach that uses specific hydrogel diffraction gratings to sense C-Reactive Protein at levels in the clinical levels. For this, a phosphorylcholine-hydrogel-based surface relief grating, produced on a laser-generated master, has been designed for the specific label-free detection of C-reactive protein in blood serum. The hydrogel is easily fabricated, and the detection is carried out with a simple optical measurement platform, constituting a reliable, easy to construct, and cheap system. This is to our knowledge the first time that direct label-free analyte detection is achieved in real samples, with sensitivity values in the clinical values of interest.

## 2. Materials and methods

### 2.1.Materials

Acrylamide (AAm), N,N′-methylenebis(acrylamide) (MBA), 2-methacryloyloxyethyl phosphorylcholine (MPC), potassium persulfate (KPS), Albumin from bovine serum ≥ 98% lyophilized powder (BSA), C-Reactive protein from human plasma (CRP), anti-mouse IgG-gold antibody produced in goat (AuNP@Ab), ERM-DA474_IFCC certified human serum (CRP),[44] human serum, potassium phosphate dibasic, potassium phosphate monobasic, sodium chloride, potassium chloride and tween-20 were purchased from Sigma-Aldrich (Madrid, Spain). Alexa Fluor® 647 NHS Ester and mouse anti-CRP antibody (anti-CRP) were purchased from ThermoFisher Scientific (Madrid, Spain). Labelled bioreagents were prepared in the laboratory following the instructions of the

supplier. PBST-S10 buffer consists of PBS-T 10 mM pH 7,4 (potassium phosphate dibasic 0,8 mM, potassium phosphate monobasic 2 mM, sodium chloride 137 mM and potassium chloride 2,7 mM, tween-20 0,05% v/v) having 10% of human serum. Polydimethylsiloxane (PDMS) Sylgard 184 was purchased from Dow Corning (Wiesbaden, Germany). The polyethylene terephthalate (PET) sheets modified with cyclohexane dimethanol (CHDM), formally denoted as PET-G, were purchased from Nudec S.A (Spain). The addition of CHDM enhances not only both the mechanical properties and chemical resistance of PET, but also its transparency in the visible spectrum. Although PET-G has a negligible absorption coefficient for wavelengths in the visible range, this material can be processed with laser radiation at wavelengths in the UV spectral range where it shows a strong absorption characterized by a high absorption coefficient (~$5\times10^5$ $cm^{-1}$) at a wavelength of 260 nm[45] useful for being treated with a laser emitting in the deep-UV wavelengths.

### 2.2.Methods

***Scanning Electron Microscopy (SEM).*** The hydrogel microstructures were analyzed by SEM using a Gemini SEM 500 system (Zeiss). First, hydrogels were completely swollen in distilled water and frozen at -20°C. Then, they were lyophilized overnight in a Telstar Lyoquest freeze-drier to yield dry aerogel samples. Finally, the dry aerogel samples were prepared for SEM analysis, just before they were analyzed, by sputter coating with an Au layer of about 15 nm in a BAL-TEC SCD 005 sputter coater (Leica microsystems).

***Optical microscopy.*** PET and PDMS masters and CRP-Sensing hydrogel gratings were characterized by optical microscopy (LEICA MICROSYSTEMS, *MZ APO).* The periods of the gratings were calculated from their cross-section profile obtained after analyzing the optical images with the ImageJ software.

***Atomic force microscopy (AFM).*** The CRP-Sensing hydrogel gratings were characterized with the peak force quantitative nanomechanical mapping mode of AFM (Multimode 8, Bruker) in water using a silicon tip (SNL-10, 0.12 N $m^{-1}$). A piece of 4 x 4 x 2 mm of the hydrogel grating was pasted onto the AFM sample holder and cover with the probe holder for scanning in liquids. Water was used as solvent and measurements were performed at room temperature.

***Fluorescence measurements.*** Alexa Fluor® 647 emission was measured with a homemade surface fluorescence reader (SFR) equipped with a CCD camera.[46] Image data processing was performed with the GenePix Pro 4.0 software (Axon Instruments, Foster City, CA, USA).

***Swelling studies.*** Lyophilized hydrogel samples were used for the swelling studies. Samples with a size of approximately 1 cm were immersed in PBS-T (10 mL) at room temperature. The weight of the swollen hydrogels was recorded at different times until they were totally swollen (reaching of constant weight). Water excess on the surface of the hydrogel was removed with a filter paper before weighing. The swelling degree was calculated from equation (1), where $W_t$ is the weight of the hydrogel after being immersed in water during time "t" and $W_0$ is the weight of the lyophilized hydrogel before the immersion.

$$\%_{Swelling} = \frac{W_t - W_0}{W_0} \times 100 \qquad (1)$$

### 2.3.Synthesis of CRP-Sensing hydrogel

AAm (380 mg), MBA (15 mg) and MPC (83 mg) were dissolved in 2 mL of $H_2O$ with 1% v/v of tween-20 and stirred for 1.5 h at r. t. Then, KPS (20 mg) was added, and the solution was sonicated for 2 minutes. Then, the mixture was poured in a glass vial (2 cm diameter). After 10 min of low vacuum application, the hydrogel was thermal cured at 70

°C for 2h. Once polymerized, the hydrogel was peeled off and washed by immersion in distilled water during at least 2 h. The water was changed at least three times to ensure that any unreacted monomers and initiator were eliminated. The hydrogels were stored at 4 ºC.

### 2.4.Fluorescence analysis of protein recognition

C-reactive protein from human plasma and albumin from bovine serum were labeled with Alexa Fluor® 647 dye, following the protocol recommended by the supplier, yielding BSA-Alexa$_{647}$ and CRP-Alexa$_{647}$. Hydrogels were cut in square pieces of 4 x 4 x 2 mm. For the optimization of the incubation time, different pieces of the hydrogel were incubated with 50 µL of labeled BSA-Alexa$_{647}$ or CRP-Alexa$_{647}$ proteins at 50 mg $L^{-1}$ in PBST-S10 for 2, 4, 6, 8, 10 and 12 h. Subsequently, they were removed from the solution and placed on a glass slide for fluorescence analysis. For the optimization of the washing time, different pieces of the hydrogel were incubated with 50 µl of labeled BSA-Alexa$_{647}$ and CRP-Alexa$_{647}$ proteins at 50 mg $L^{-1}$ in PBST-S10 for 4 h and washed with PBS-T for different times (14 (overnight), 18, 20, 22 and 24 h). Every washing step implied a change of the washing solution; for example, washing for 14 h had 1 change of the washing solution while washing for 24 h had 5 changes. Subsequently, they were removed from the PBST-S10 solutions and placed on a glass slide for fluorescence analysis. Once the incubation and washing times were optimized, different pieces of the hydrogels were incubated with 50 µl of solutions of labeled BSA-Alexa$_{647}$ or CRP-Alexa$_{647}$ proteins at 0, 25, 50, 100, 200, 300 and 400 mg $L^{-1}$ in PBST-S10 during 4 h. Then, hydrogels were washed overnight with PBS-T. Subsequently, they were removed from the solution and placed on a glass slide for fluorescence analysis. The fluorescence of all samples was

224 registered and the signal intensity was quantified with the GenePix Pro 4000B software
225 ($\lambda_{ex}$=633 nm, $\lambda_{em}$=670 nm). All experiments were repeated three times.
226
227 **2.5.Fabrication of the grating masters**
228 Grating masters were fabricated using the Direct Laser Interference Patterning (DLIP)
229 technology.[47] For this work, a frequency quadrupled Q-switched laser head (Laser-export
230 Co. Ltd., TECH-263 Advanced) with a maximum pulse energy of 50 µJ and operating at
231 a wavelength of 263 nm and a pulse duration shorter than 3 ns was used. The laser beam
232 has a Gaussian intensity distribution (TEM00) with a beam quality of $M^2 < 1.3$. The
233 structuring of the PET-G samples was conducted by a compact two-beam DLIP system
234 (Fraunhofer IWS, Figure 1a). It produces confined DLIP treated areas per laser pulse
235 containing line-like structures with a selected periodicity within a diameter of ~25 µm.
236 The optical configuration allows the fully automatic control of the spatial period Λ
237 between 1.5 µm – 11.0 µm by varying the angle of incidence of the beams on the sample
238 (Figure 1b). In this work, gratings with a spatial period of 3.0 µm were fabricated by
239 setting the interference angle to 2.51°. To create areas larger than the DLIP pixel, the
240 sample is precisely moved by a stage system (PRO155-05, Aerotech GmbH, Fürth,
241 Germany), resulting in square-shaped processed areas with an edge length of 20 mm
242 homogeneously covered with the line-like pattern. In particular, the samples were moved
243 in the direction parallel to the interference lines with a spatial pulse separation p = 16.7
244 µm and successively displaced laterally of a quantity h = 3µm (hatch distance), chosen as
245 an integer of the spatial period (Figure 1c). A laser fluence of 0.13 J/cm² was applied.

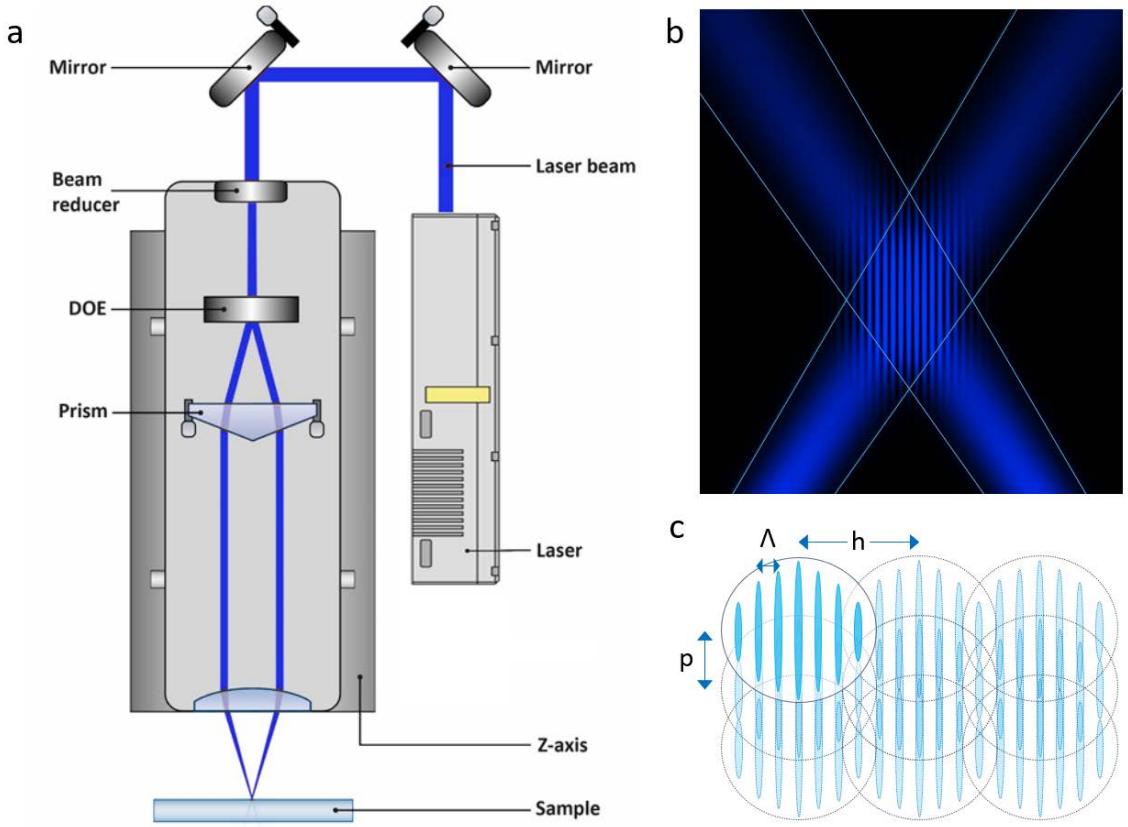


**Figure 1**. **(a)** Schematic representation of the DLIP optical setup, **(b)** depiction of the interference effect between two Gaussian laser beams overlapping and **(c)** sample processing scheme showing the displacement of DLIP pixels on the sample's surface. The scanning direction is vertical.

### 2.6.Fabrication of the CRP-Sensing hydrogel gratings

CRP-Sensing hydrogel gratings were fabricated through the replication of a PDMS master obtained from the PET-G master. A liquid mixture of PDMS was poured onto the structured side of the PET-G master, removing bubbles with low vacuum for at least 15 min. After that, polymerization took place overnight at 60 ºC. The polymerized PDMS master was peeled off and used as a template for the fabrication of the holographic hydrogel. 2 mL of the monomer solution with KPS (see synthesis of the hydrogel section) was drop-cast onto the structured side of the PDMS master placed on small vial (2 cm diameter). After vacuum purge for 10 min, the holographic hydrogel was cured for 2 h at

70 ºC. Once polymerized, it was peeled off and washed by immersion in distilled water during at least 2 h, using three times fresh water to ensure that non polymerized monomers were eliminated. The hydrogels were stored at 4 ºC.

### 2.7.Measurement setup

Figure 2 shows the experimental setup used for the biosensing and for the characterization of the different structured materials (*i.e.* diffraction efficiency or zero/1$^{st}$ diffraction order distances) (See also figure S1). From the bottom to the top, a laser beam (650 nm) is orthogonally directed towards an adjustable diaphragm to the sample holder (opening = 2 mm). The sample holder has been home made to host a 96-well plate and to facilitate its 2D movement in a horizontal way (x and y dimensions). A movable plane concave spherical lens (f = 30 mm) is placed on the top of the 96-well plate to focus the diffracted beams. The intensity and the number of orders that can be observed after the diffraction of the light by the gratings depend on the structural characteristics of the gratings as well as on the fabrication material itself (*i.e.* PDMS, PET-G or hydrogel). In this work, only the zero and first diffraction orders are considered. A movable silicon photodiode is placed after the lens to record the intensity of the incident light (no sample on the holder) or the zero diffraction order (with a sample placed on the holder). A second movable silicon photodiode is placed at certain angle of the incident laser beam to monitor the intensity of the first diffraction order. The generated current is converted into voltage by the resistors connected to the photodiodes (75 and 3400 kΩ for zero and first diffraction order intensities, respectively). The diffraction efficiency of the gratings, *i.e.* the analytical signal, is obtained from the intensity ratios of the first and zero order diffraction beams (equation 2).

$$DE\ (\%) = \frac{I_1}{I_0} \times 100 \quad (2)$$

Where *DE* is the diffraction efficiency for the first diffraction order, $I_1$ is the intensity of the first order diffraction beam an $I_0$ is the intensity of the zero order diffraction beam. Besides, a white screen equipped with a ruler is placed on the top of the system to hold the projection of the entire diffraction pattern of the gratings (D = 1000 mm from the sample holder). Finally, a digital camera (Nikon, D3200) is placed at a fixed distance from the white screen to register the diffraction patterns. The first diffraction order in gratings is governed by equation (3)[48] which, for small diffraction angles, can be simplified in equation (4) to correlate the period of the gratings with the distance between the diffracted orders:

$$\Lambda = \frac{\lambda}{sin\theta} \quad (3) \qquad\qquad \Lambda = D\frac{\lambda}{y} \quad (4)$$

where $\Lambda$ is the period of the grating, $\lambda$ is the wavelength of the incident beam, $\theta$ is the incident angle from sample normal, *D* is the distance between the screen and the sample and *y* is the distance between the first and zero orders.

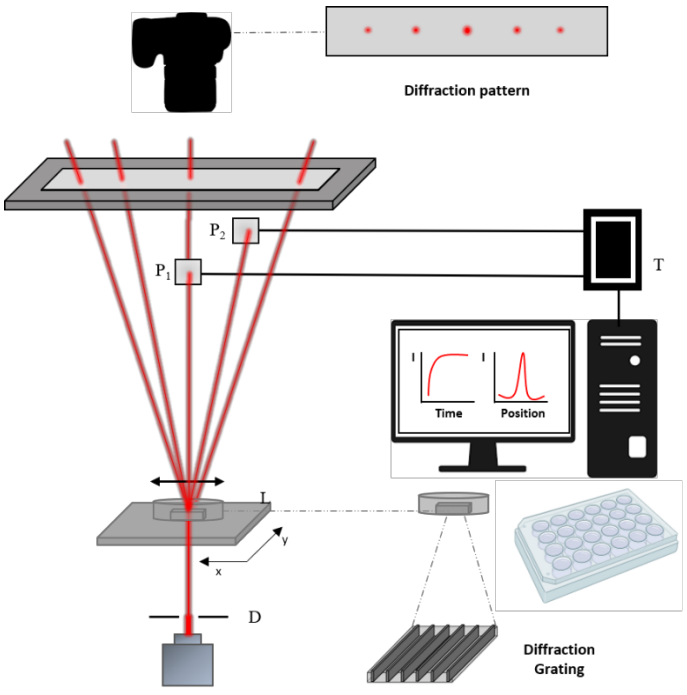

**Figure 2.** Scheme of the measurement set-up, L: movable lens; D: diaphragm. P: movable photodiodes; T: Transductor.

### 2.8. Characterization of fabricated diffraction gratings with the optical setup

A portion of a PET-G master, a PDMS master or a CRP-Sensing hydrogel grating, with the surface diffraction grating on the upper face, was placed on a glass slide onto the sample holder. After irradiation with the laser beam (650 nm), the diffraction patterns of the gratings projected on the white screen placed at a fixed distance (1000 mm) were registered with the digital camera and the images were analyzed with the ImageJ software. The distance between the diffraction spots was used to calculate the grating periods using equation 3.

### 2.9. Label-free biosensing of CRP using hydrogel gratings

Several CRP-Sensing hydrogel gratings (dimensions: 4x4x2 mm), with the surface diffraction grating on the upper face, were placed in different wells of a transparent 96 well-plate. Firstly, a defined volume (300 µL) of PBS-T was added in each well and the 96 well-plate was stirred in an orbital stirrer for 14 h for the homogenization of the hydrogels on the measurement medium. After that, PBS-T solution was discarded and 100 µL of fresh PBS-T were added for the initial diffraction measurements. The amount of PBS-T was enough to allow the patterned surface of the hydrogel to be totally immersed in the liquid.

Protein samples (CRP and BSA) with different concentrations in the 1-50 mg $L^{-1}$ range were prepared in PBST-S10 medium. Furthermore, two samples of CRP in certified serum were prepared by dilution of the standard solution in PBS-T (dilution factors: 1/10 and 1/2). After the initial diffraction measurements, the PBS-T solution was discarded,

and hydrogels were incubated at room temperature with 50 µL of protein samples for 4 h. Then, protein samples were discarded, 300 µL of PBS-T were added, and finally the 96 well-plate was stirred in an orbital stirrer for 14 h. After that, PBS-T solutions were discarded and 100 µL of fresh PBS-T were added for the final diffraction measurements. Zero and first order diffraction intensities were recorded with the optical measurement setup. The relative diffraction efficiency (respect to the initial diffraction efficiency) was used to characterize the protein-sensing response of the hydrogels, as described in equation 5:

$$RDE(\%) = \frac{DE_f - DE_i}{DE_i} \times 100 \qquad (5)$$

where *RDE* is the relative diffraction efficiency, $DE_i$ is the initial diffraction efficiency (after the homogenization step with PBS-T) and $DE_f$ is the final diffraction efficiency (after incubation and washing steps) for the first diffraction order. All experiments were repeated three times.

On the other hand, after the steps of incubation with protein samples and diffraction measurements, CRP-Sensing hydrogel gratings were incubated at room temperature with 50 µL of anti-CRP antibody in PBST-S10 (50 mg $L^{-1}$) for 4 h for signal amplification. After washing with 300 µL of PBS-T for 14 h, the PBS-T was replaced with 100 µL of PBS-T and the diffraction intensities were registered. A second amplification step was carried out by addition of 50 µL of anti-mouse IgG modified gold nanoparticles in PBST-S10 (AuNP@Ab, dilution factor: 1/20), to the samples previously incubated with anti-CRP, incubation for 4 h at room temperature and washing with 300 µL of PBS-T for 14 h. The diffraction intensities were registered after replacing the PBS-T with 100 µL of fresh PBS-T. RDE was calculated for both amplification steps according to equation 5.

## 3. Results and discussion

### 3.1.Hydrogel synthesis

Uncountable combinations of monomers, crosslinkers, and initiators have been studied over the years to obtain hydrogels for different applications. Choosing the composition is not trivial as the macroscopic characteristics and properties of the hydrogels are directly affected by their starting components. Transparency, porosity, mechanical stability, and malleability are the key requirements for applying hydrogels as surface relief gratings suitable for sensing. In addition, they should be smartly functionalized with a recognition element that allows selective detection of the analyte of interest without significantly compromising these key requirements.

The objective of this work is the selective detection of C-Reactive protein and, for this purpose, a phosphocholine moiety as recognition element was used. Besides, the selected molecule, 2-methacryloyloxyethyl phosphorylcholine (MPC), bears an acrylate modification that allows its polymerization within the hydrogel matrix. Looking for transparency and improved mechanical properties, acrylamide (AAm) was chosen as the skeleton monomer of the hydrogel because polyacrylamide hydrogels show high optical properties.[49] Indeed, AAm is among the most utilized monomers in the synthesis of holographic and photonic hydrogels which also need high transparency and stability.[50] N,N′-methylenebisacrylamide (MBA) was chosen as the most common binder for polyacrylamide hydrogels, and hydrogels were synthesized by *in situ* radical polymerization using KPS as the thermal initiator (Figure S2, Supporting Information).

Figure 3a shows the digital image of the bulk hydrogel in its swollen state in water (zenith angle). As it can be seen, the obtained material is completely transparent, and the hydrogel was mouldable. Figure 3b shows the microscopic morphology of the same hydrogel studied by Scanning Electron Microscopy. The hydrogel shows a homogeneous and

porous mesh with a tight entanglement structure due to the high concentration of crosslinking centers. Hydrogels exhibits 800% swelling degree in PBS-T (Figure S3, Supporting Information).

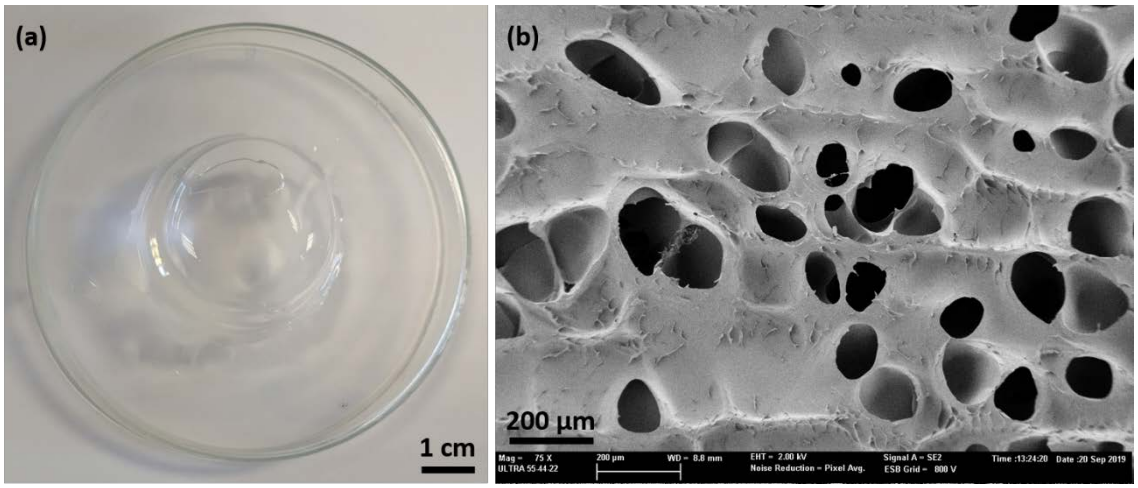


**Figure 3. (a)** Digital image of the CRP-Sensing hydrogel in its swollen state and **(b)** SEM image of the lyophilized CRP-Sensing hydrogel.

### 3.2.Fluorescence analysis of protein recognition

Before assessing the capacity of the hydrogel to act as a surface relief grating based transducer in biosensing, its capacity to recognize the CRP was analyzed by fluorescence spectroscopy. To achieve that, proteins were labeled with Alexa647 dye following the instructions of the supplier. As the major aim is the detection of the protein in blood serum, all the solutions used in the experiments were prepared in PBS-T diluted with 10% of human serum (PBST-S10). The human serum does not only mimic the real environment of the CRP protein, but also provide the medium with $Ca^{2+}$ ions that are needed for the effective interaction between the phosphorylcholine units and the CRP.[51] All the designed experiments were also carried out with BSA to assess the selectivity of the system. Figure 4a shows the fluorescence signal of hydrogels after their incubation

393 with labeled BSA-Alexa$_{647}$ or CRP-Alexa$_{647}$ at 50 mg $L^{-1}$ in PBST-S10 at different
394 incubation times. The results show that both proteins can diffuse across the hydrogel
395 matrix and the signal is stable after 4h of incubation. The high fluorescence signal at 2h
396 of incubation can be due to an accumulation of proteins at the border of the material at
397 shorter times. Figure 4b shows the relative fluorescence intensity of the hydrogels
398 incubated with labeled BSA-Alexa$_{647}$ or CRP-Alexa$_{647}$ at 50 mg $L^{-1}$ in PBST-S10 for 4h
399 after washing with PBS-T for different times. The results show that BSA-Alexa$_{647}$ is
400 virtually removed after overnight washing while CRP-Alexa$_{647}$ is retained by the hydrogel
401 matrix even after 24 h of washing. Figure 4c shows the binding curve of hydrogels
402 incubated with increasing concentrations of labeled BSA-Alexa$_{647}$ or CRP-Alexa$_{647}$ at the
403 previously optimized incubation and washing time. Data were fitted to a sigmoidal
404 (logistic 4 parameters) regression ($R^2$=0.996). The increase in the fluorescence signal is
405 proportional to the concentration of the target CRP-Alexa$_{647}$ while almost no signal is
406 observed for BSA-Alexa$_{647}$ even at 400 mg $L^{-1}$ (Figure S4, Supporting Information).
407 Therefore, the hydrogel designed here is a suitable material to develop biosensors specific
408 for CRP protein determination.

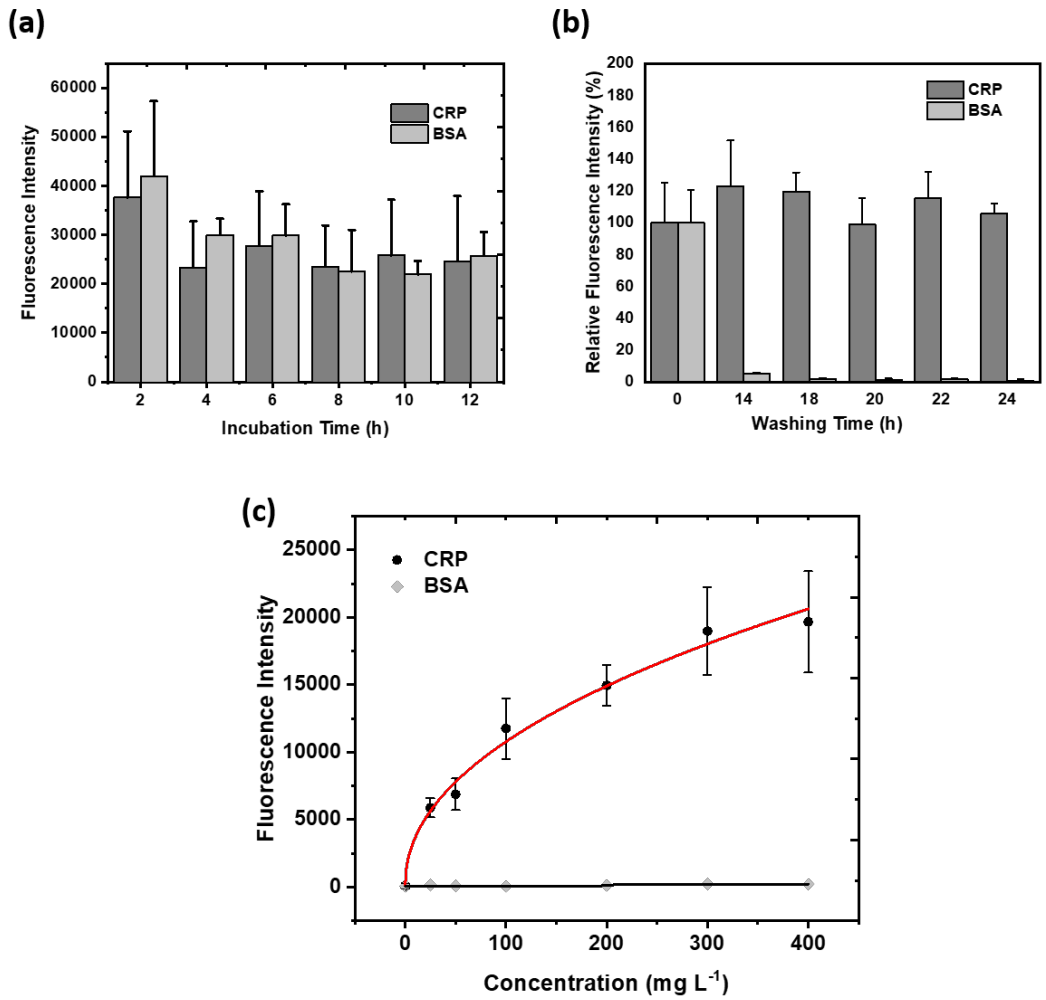


**Figure 4. (a)** Fluorescence intensity of hydrogels incubated with labeled BSA-Alexa$_{647}$ or CRP-Alexa$_{647}$ at 50 mg L$^{-1}$ in PBST-S10 at different incubation times. **(b)** Relative fluorescence intensity of hydrogels incubated with BSA-Alexa$_{647}$ or CRP-Alexa$_{647}$ at 50 mg L$^{-1}$ in PBST-S10 after washing with PBS-T for different times. **(c)** Binding curves for hydrogels incubated with increasing concentrations of BSA-Alexa$_{647}$ or CRP-Alexa$_{647}$ in PBST-S10 for 4 h after washing for 14 h with PBS-T. All experiments were repeated three times.

### 3.3.Fabrication and characterization of PET-G and PDMS masters and CRP-Sensing hydrogel gratings

Once the suitability of the hydrogels for selectively recognize CPR protein was demonstrated, surface relief grating transducers of this material were fabricated. For this purpose, the first step was the production of a mother master by DLIP using a PET-G substrate.[47] Thanks to the interference effect, DLIP is useful for building well defined and almost defect-free periodic structures in different geometries. Thermoplastic (i.e. PET) are preferred to metal masters since thermoplastics are resistant to most organic solvent, acid and bases. Moreover, thermoplastic are soft materials which facilitates the demolding process after replication without damaging the substrates. Conditions were chosen to obtain masters with line-like periodic features having a period of 3 μm. Then, a PDMS master with the negative structure of the PET-G stamp was prepared by replica moulding. Subsequently, the CRP-Sensing hydrogel gratings were fabricated by soft-lithography from the PDMS master. Vacuum and polymerization times were optimized to obtain homogeneous materials (data not shown).

Diffraction of the CRP-Sensing hydrogel gratings was characterized with the optical setup and compared with the diffraction of the PDMS and the PET-G masters. Figure 5a shows the diffraction pattern of the CRP-Sensing hydrogel. The grating period calculated for this grating was 3790 ± 90 nm while the ones obtained for the diffraction patterns of the PDMS master and PET-G gratings (Figure S5, Supporting Information) were 3050 ± 10 nm and 3020 ±10 nm, respectively. As expected, the grating period of the CRP-Sensing hydrogel was larger than the ones of the PDMS and PET-G masters due to the swelling produced in the hydrogel matrix after the immersion in water. The relative errors associated with the diffraction measurements of the grating periods are less than 3%. Moreover, the grating periods calculated by diffraction measurements are in good agreement with those directly determined by optical microscopy (Figure 5b and c and Figure S6, Supporting Information). From these images, the grating periods were

estimated to be 3720 ± 70 nm for the CRP-Sensing hydrogel and 2890 ± 50 nm and 3000 ± 40 nm and for the PDMS and PET-G masters, respectively. Figure 5d shows the AFM image of the CRP-Sensing hydrogel obtained in water where a grating period of approximately 3.7 µm can be observed in a three-dimensional view. All these data confirm the correct replication of the gratings. It should be noticed that the AFM image cannot be used for the analysis of the depth of the gratings as the aspect ratio and shape of the measure grooves prevents the correct approaching of the tip of the cantilever to their deepest bottom.[52]

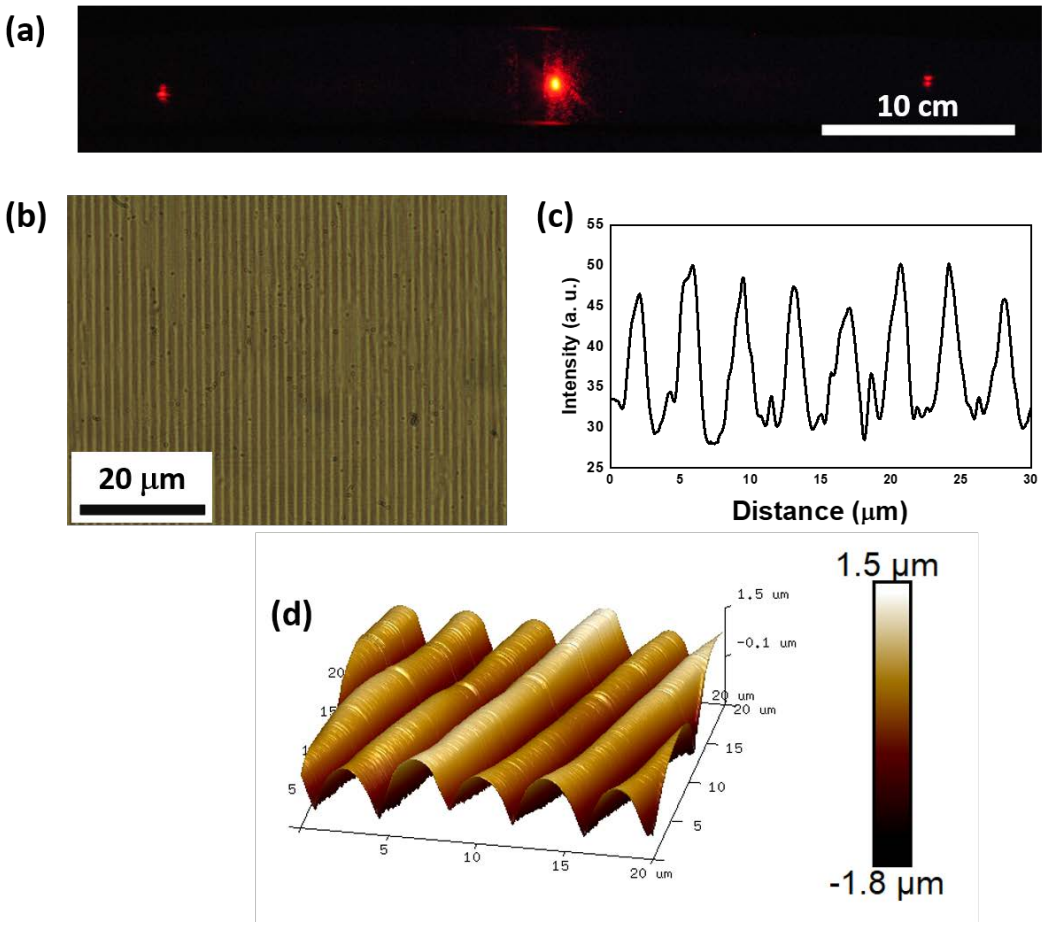


**Figure 5.** Characterization of the CRP-Sensing hydrogel immersed in water. **(a)** Diffraction pattern projected on a white screen after irradiation of the hydrogel grating with a laser beam of 650 nm. **(b)** Optical microscopy image, **(c)** cross section profile of

457 the optical image (intensity in the abscissa refers to the mean gray value obtained from
458 optical images analyzed with the ImageJ software) and **(d)** AFM image.
459
460 **3.4.Label-free biosensing of CRP using hydrogel gratings**
461 The response of the label-free CRP-Sensing hydrogels was characterized by their
462 incubation with solutions of CRP and BSA at different concentrations, from 0 to 50 mg
463 $L^{-1}$ in PBST-S10. For that, hydrogel gratings were placed in the wells of a 96 well-ELISA
464 plate, incubated with the protein solution, and washed. The diffraction effect was visible
465 by naked eyed in the hydrogels under illumination with normal room white light (Figure
466 S7, Supporting Information). The zero and first diffraction order beam intensities were
467 registered with the measurement optical setup showing stability for at least 30 minutes
468 (Figure S8, Supporting Information), therefore, slight delays in the reading time would
469 not affect to the obtained results. Figure 6a shows the relative diffraction efficiencies of
470 the CRP-Sensing hydrogels after the assay with protein samples at different
471 concentrations. Incubation and washing times were selected as the optimized in the
472 fluorescence analysis, 4 and 14 h, respectively. The RDE values of hydrogels increase
473 with the concentration of CRP, while they remain practically invariable after incubation
474 with BSA. The results show that the hydrogels exhibit a specific response to the CRP in
475 the tested concentration range. The data can be best fitted by a dose-response type
476 sigmoidal correlation curve, obtaining a correlation coefficient of $R^2 = 0.988$. Limits of
477 detection (LOD) and quantification (LOQ) of 1.07 and 8.92 mg $L^{-1}$, respectively, were
478 obtained from this curve. Concentrations of CRP in human serum from healthy adults are
479 normally around 0.8 mg $L^{-1}$,[53] and levels higher than 10 and 50 mg $L^{-1}$ in plasma are
480 indicative of risk of developing a fatal CVD[54] or sepsis,[55] respectively. Therefore, the

results show that our system could be used for the detection of these risks in human samples.

The diffraction efficiency of thin gratings at fixed wavelength and their Bragg angle can be directly correlated to the refractive index modulation of the gratings. Therefore, the increase in the RDE of the hydrogel gratings incubated with CRP can be ascribed to an increase of the refractive index modulation of the gratings after the specific recognition of the CRP by the hydrogel through the polymer chains bearing the MPC moiety. The decrease of the dose-response curve slope at high CRP concentrations can be attributed to the saturation of the protein adsorption on the surface of the hydrogels.

### 3.5. Amplification strategies

Amplification strategies were designed to evaluate if a higher increase of the refractive index modulation of the gratings and, thus, an improvement of the analytical performance of the biosensing system could be achieved. Hydrogels previously incubated with CRP samples at increasing concentrations were subsequently incubated with anti-CRP antibody (50 mg $L^{-1}$) and then with anti-mouse IgG-gold antibody (AuNP@Ab, dilution factor: 1/20) in PBST-S10. The RDE (%) of the hydrogels after incubation with every sample are shown in Figure 6b. The data were fitted by linear correlation curves ($R^2$ = 0.986 and $R^2$ = 0.983 for amplifications with anti-CRP and AuNP@Ab antibodies, respectively). RDE values increase after the amplification steps for hydrogels incubated with protein solutions at the whole tested concentration range. The amplification steps yielded a wider linear dynamic range than the direct assay for the tested concentration range. In addition, the detection and quantification limits decreased, while sensitivity increased after the amplification steps. LOD were 0.51 and 0.30 mg $L^{-1}$ for anti-CRP and AuNP@Ab antibody amplification, respectively, LOQ were 4.36 and 5.31 mg $L^{-1}$ for

anti-CRP and AuNP@Ab antibody amplifications, and sensitivities were 2.9 and 3.8 % L $mg^{-1}$ for anti-CRP and AuNP@Ab antibody amplifications, respectively. Therefore, amplifications strategies could be useful tools for improving the analytical performance of our initial biosensing system to not only detect but quantify lower concentrations of CRP reaching the requirements for what is known as high-sensitivity CRP (hs-CRP), which has an independent predictive potential cardiovascular risk factor (ranging from 1 to 3 mg $L^{-1}$).

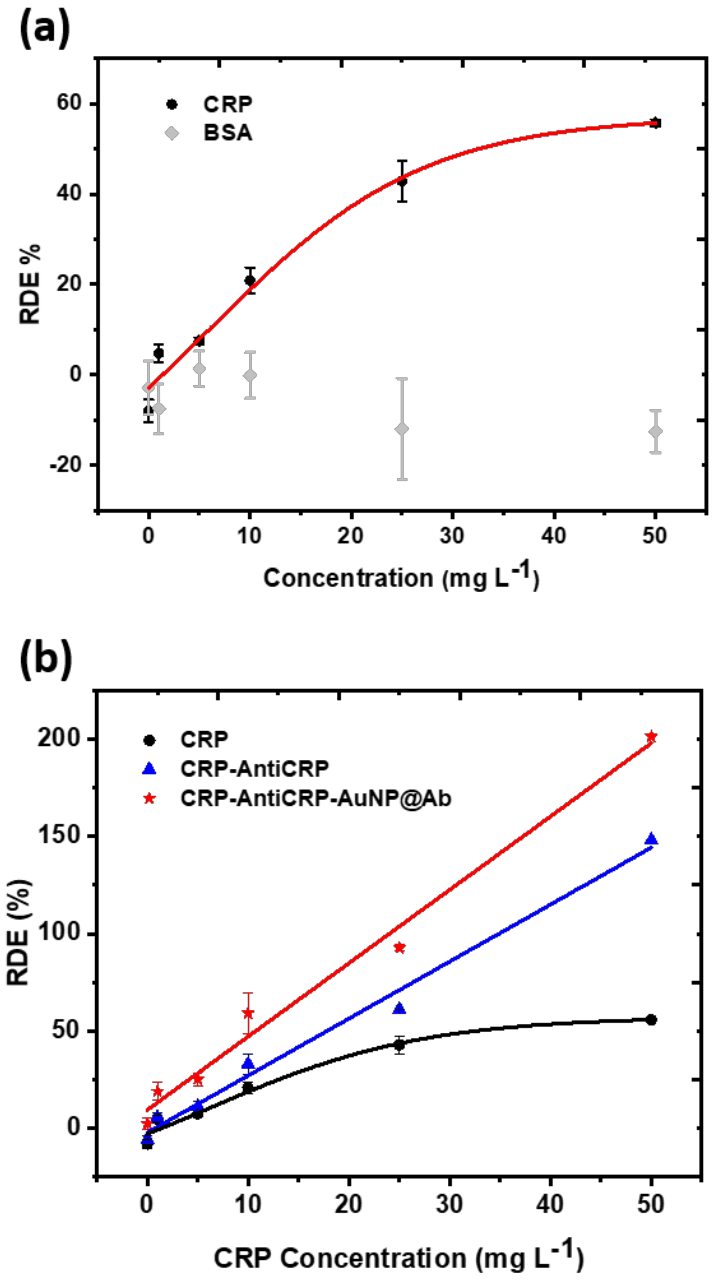

**Figure 6. (a)** Binding curves for CRP-Sensing hydrogel gratings incubated with increasing concentrations of BSA or CRP in PBST-S10 for 4 h after washing for 14h with PBS-T. **(b)** Binding curves for CRP-Sensing hydrogel gratings incubated with CRP, with CRP and anti-CRP antibody and with CRP, anti-CRP and AuNP@Ab antibodies. All experiments were repeated in triplicate.

### 3.6.Detection of CRP in a certified human serum sample

With the purpose to demonstrate the capability of our system to analyze real samples, CRP in a certified human serum was determined using the different biosensing strategies here proposed. Certified human serum was 1/10 and 1/2 diluted with PBS-T and measured in our system. Table 1 shows the calculated concentrations, obtained by interpolation from the corresponding calibration curves. Analysis of samples at a 1/10 dilution factor yielded accurate results but with recoveries around 130%, which is slightly over the accepted values in immunoassay (80%-120%). These results can be ascribed to the fact that the signals obtained at those dilutions fall nearly out of the dynamic range of our calibration curves. The direct assay of samples with a 1/2 dilution is not either recommended as it also falls out of the linear interval. Nevertheless, recoveries around 100% were obtained for samples with a 1/2 dilution factor analyzed with the amplification strategies. The data demonstrate that working with blood serum is possible at two levels of dilution and the system results specific for CRP, not being affected by the rest of proteins and blood components. Successful detection of CRP was achieved with all the biosensing strategies, but further improvements would be interesting for quantification at high dilutions.

| Biosensing strategy | Dilution factor* | | | | |
|---|---|---|---|---|---|
| | 1/10 | | 1/2 | | |
| | Expected concentration (mg $L^{-1}$) | Detected concentration mg $L^{-1}$) | Expected concentration (mg $L^{-1}$) | Detected Concentration (mg $L^{-1}$) | Recovery range (%) |
| Label-Free | 4.12 | 5.39 ± 0.02 | 20.06 | -*[a] | -*[a] |
| Anti-CRP antibody | 4.12 | 5.77 ± 0.01 | 20.06 | 20 ± 3 | 96-113 |
| AuNP@Ab antibody | 4.12 | 5.30 ± 0.04 | 20.06 | 22 ± 2 | 100-113 |

**Table 1.** Determination of CRP in certified human serum using different biosensing strategies: Calculated concentration from the different fitted data and recovery factors. *Certified Human serum contains 41.2 mg $L^{-1}$ of CRP. All experiments were repeated three times.

*[a]: out of the linear range.

## 4. Conclusions

A novel biosensing system based on bioresponsive hydrogel-based surface relief gratings has been developed. The appropriate design of the hydrogels has allowed the label-free and selective detection of CRP at a suitable concentration range for clinical applications using a homemade optical measurement setup. The biosensing system allows the application of amplification strategies to improve its analytical performance. In addition, determination of CRP in certified serum has been carried out and recoveries up to 100% have been obtained. As the measurements are demonstrated using a 96-wells ELISA plate, the high-throughput screening potential of the approach is high. Also, it paves the way to further developments with other analytes, or amplification strategies, being a cheap and appealing approach where no micro/nanofabrication facilities, neither complicated optical systems are required to implement it.

## Notes

The authors declare no competing financial interest.


## Acknowledgement

This work was financially supported by the E.U. FEDER, the Spanish Ministry of Economy and Competitiveness MINECO (BiHolog-CTQ2016-75749-R and AdBiHol-PID2019-110713RB-I00) and Generalitat Valenciana (PROMETEO/2020/094). M. I. Lucío acknowledges MINECO for her Juan de la Cierva Formación and Incorporación grants (FJCI-2016-29593, IJC2018-035355-I). The authors acknowledge the assistance and advice of the Electron Microscopy Service of the Universitat Politècnica de València.


## Bibliography


(1) Goh, J. B.; Loo, R. W.; McAloney, R. A.; Goh, M. C. Diffraction-Based Assay for Detecting Multiple Analytes. *Anal. Bioanal. Chem.* **2002**, *374* (1), 54–56. https://doi.org/10.1007/s00216-002-1478-5.

(2) Goh, J. B.; Loo, R. W.; Goh, M. C. Label-Free Monitoring of Multiple Biomolecular Binding Interactinos in Real-Time with Diffraction-Based Sensing. *Sensors Actuators B* **2005**, *106*, 243–248.

(3) Avella-Oliver, M.; Carrascosa, J.; Puchades, R.; Maquieira, Á. Diffractive Protein Gratings as Optically Active Transducers for High-Throughput Label-Free Immunosensing. *Anal. Chem.* **2017**, *89* (17), 9002–9008. https://doi.org/10.1021/acs.analchem.7b01649.

(4) Avella-Oliver, M.; Ferrando, V.; Monsoriu, J. A.; Puchades, R.; Maquieira, A. A

Label-Free Diffraction-Based Sensing Displacement Immunosensor to Quantify Low Molecular Weight Organic Compounds. *Anal. Chim. Acta* **2018**, *1033*, 173–179. https://doi.org/10.1016/j.aca.2018.05.060.

(5) Juste-Dolz, A.; Delgado-Pinar, M.; Avella-Oliver, M.; Fernández, E.; Pastor, D.; Andrés, M. V.; Maquieira, Á. BIO Bragg Gratings on Microfibers for Label-Free Biosensing. *Biosens. Bioelectron.* **2021**, *176*, 112916. https://doi.org/10.1016/j.bios.2020.112916.

(6) Juste-Dolz, A.; Avella-Oliver, M.; Puchades, R.; Maquieira, A. Indirect Microcontact Printing to Create Functional Patterns of Physisorbed Antibodies. *Sensors* **2018**, *18* (9), 3163. https://doi.org/10.3390/s18093163.

(7) Wang, X.; Wang, X. Aptamer-Functionalized Hydrogel Diffraction Gratings for the Human Thrombin Detection. *Chem. Commun.* **2013**, *49* (53), 5957–5959. https://doi.org/10.1039/c3cc41827h.

(8) Waller, E. H.; Dix, S.; Gutsche, J.; Widera, A.; von Freymann, G. Functional Metallic Microcomponents via Liquid-Phase Multiphoton Direct Laser Writing: A Review. *Micromachines* **2019**, *10* (12), 1–17. https://doi.org/10.3390/mi10120827.

(9) Alqattan, B.; Yetisen, A. K.; Butt, H. Direct Laser Writing of Nanophotonic Structures on Contact Lenses. *ACS Nano* **2018**, *12* (6), 5130–5140. https://doi.org/10.1021/acsnano.8b00222.

(10) Lasagni, A. F.; Alamri, S.; Aguilar-Morales, A. I.; Rößler, F.; Voisiat, B.; Kunze, T. Biomimetic Surface Structuring Using Laser Based Interferometric Methods. *Appl. Sci.* **2018**, *8* (8), 1260. https://doi.org/10.3390/app8081260.

(11) Lasagni, A. F.; Kunze, T.; Bieda, M.; Günther, D.; Gärtner, A.; Lang, V.; Rank, A.; Roch, T. Large Area Micro-/Nano-Structuring Using Direct Laser Interference Patterning. *Proc. Vol. 9735, Laser Appl. Microelectron. Optoelectron. Manuf. XXI* **2016**, *97351*, 973515.

(12) Rößler, F.; Kunze, T.; Lasagni, A. F. Fabrication of Diffraction Based Security Elements Using Direct Laser Interference Patterning. *Opt. Express* **2017**, *25* (19), 22959. https://doi.org/10.1364/oe.25.022959.

(13) Soldera, M.; Alamri, S.; Sürmann, P. A.; Kunze, T.; Lasagni, A. F. Microfabrication and Surface Functionalization of Soda Lime Glass through Direct Laser Interference Patterning. *Nanomaterials* **2021**, *11*, 129. https://doi.org/10.3390/nano11010129.

(14) Storm, S.; Alamri, S.; Soldera, M.; Kunze, T.; Lasagni, A. F. How to Tailor Structural Colors for Extended Visibility and White Light Generation Employing Direct Laser Interference Patterning. *Macromol. Chem. Phys.* **2019**, *220*, 1900205. https://doi.org/10.1002/macp.201900205.

(15) Koetting, M. C.; Peters, J. T.; Steichen, S. D.; Peppas, N. A. Stimulus-Responsive Hydrogels: Theory, Modern Advances, and Applications. *Mater. Sci. Eng. R Reports* **2015**, *93*, 1–49. https://doi.org/10.1016/j.mser.2015.04.001.

(16) Ulijn, R. V.; Bibi, N.; Jayawarna, V.; Thornton, P. D.; Todd, S. J.; Mart, R. J.; Smith, A. M.; Gough, J. E. Bioresponsive Hydrogels. *Mater. Today* **2007**, *10* (4), 40–48. https://doi.org/10.1016/S1369-7021(07)70049-4.

(17) Micoli, A.; Quintana, M.; Prato, M. Novel Nanostructures Based on the Active Interplay between Nucleobases and Carbon Nanotubes. *Supramol. Chem.* **2013**, *25* (9–11), 567–573. https://doi.org/10.1080/10610278.2013.824577.

(18) Asher, S. A.; Alexeev, V. L.; Goponenko, A. V.; Sharma, A. C.; Lednev, I. K.; Wilcox, C. S.; Finegold, D. N. Photonic Crystal Carbohydrate Sensors: Low Ionic Strength Sugar Sensing. *J. Am. Chem. Soc.* **2003**, *125* (11), 3322–3329. https://doi.org/10.1021/ja021037h.

(19) Alexeev, V. L.; Sharma, A. C.; Goponenko, A. V.; Das, S.; Lednev, I. K.; Wilcox, C. S.; Finegold, D. N.; Asher, S. A. High Ionic Strength Glucose-Sensing Photonic Crystal. *Anal. Chem.* **2003**, *75* (10), 2316–2323. https://doi.org/10.1021/ac030021m.

(20) Dean, K. E. S.; Horgan, A. M.; Marshall, A. J.; Kabilan, S.; Pritchard, J. Selective Holographic Detection of Glucose Using Tertiary Amines. *Chem. Commun.* **2006**, No. 33, 3507–3509. https://doi.org/10.1039/b605778k.

(21) Kabilan, S.; Blyth, J.; Lee, M. C.; Marshall, A. J.; Hussain, A.; Yang, X.; Lowe, C. R. Glucose-Sensitive Holographic Sensors. *J. Mol. Recognit.* **2004**, *17*, 162–166.

(22) Horgan, A. M.; Marshall, A. J.; Kew, S. J.; Dean, K. E. S.; Creasey, C. D.; Kabilan, S. Crosslinking of Phenylboronic Acid Receptors as a Means of Glucose Selective Holographic Detection. *Biosens. Bioelectron.* **2006**, *21* (9), 1838–1845. https://doi.org/10.1016/j.bios.2005.11.028.

(23) Kabilan, S.; Marshall, A. J.; Sartain, F. K.; Lee, M. C.; Hussain, A.; Yang, X.; Blyth, J.; Karangu, N.; James, K.; Zeng, J.; et al. Holographic Glucose Sensors. *Biosens. Bioelectron.* **2005**, *20* (8 SPEC. ISS.), 1602–1610. https://doi.org/10.1016/j.bios.2004.07.005.

(24) Lee, M. C.; Kabilan, S.; Hussain, A.; Yang, X.; Blyth, J.; Lowe, C. R. Glucose-Sensitive Holographic Sensors for Monitoring Bacterial Growth. *Anal. Chem.*

652 **2004**, *76* (19), 5748–5755. https://doi.org/10.1021/ac049334n.

653 (25) Kim, J.; Singh, N.; Lyon, L. A. Label-Free Biosensing with Hydrogel
654 Microlenses. *Angew. Chemie - Int. Ed.* **2006**, *45* (9), 1446–1449.
655 https://doi.org/10.1002/anie.200503102.

656 (26) Yetisen, A. K.; Jiang, N.; Fallahi, A.; Montelongo, Y.; Ruiz-Esparza, G. U.;
657 Tamayol, A.; Zhang, Y. S.; Mahmood, I.; Yang, S. A.; Kim, K. S.; et al. Glucose-
658 Sensitive Hydrogel Optical Fibers Functionalized with Phenylboronic Acid. *Adv.*
659 *Mater.* **2017**, *29* (15). https://doi.org/10.1002/adma.201606380.

660 (27) Tierney, S.; Hasle Falch, B. M.; Hjelme, D. R.; Stokke, B. T. Determination of
661 Glucose Levels Using a Functionalized Hydrogel-Optical Fiber Biosensor:
662 Toward Continuous Monitoring of Blood Glucose in Vivo. *Anal. Chem.* **2009**, *81*
663 (9), 3630–3636. https://doi.org/10.1021/ac900019k.

664 (28) Elsherif, M.; Hassan, M. U.; Yetisen, A. K.; Butt, H. Hydrogel Optical Fibers for
665 Continuous Glucose Monitoring. *Biosens. Bioelectron.* **2019**, *137* (April), 25–32.
666 https://doi.org/10.1016/j.bios.2019.05.002.

667 (29) Ye, G.; Wang, X. Glucose Sensing through Diffraction Grating of Hydrogel
668 Bearing Phenylboronic Acid Groups. *Biosensors and Bioelectronics*. 2010, pp
669 772–777. https://doi.org/10.1016/j.bios.2010.06.029.

670 (30) Peng, H. Y.; Wang, W.; Gao, F.; Lin, S.; Liu, L. Y.; Pu, X. Q.; Liu, Z.; Ju, X. J.;
671 Xie, R.; Chu, L. Y. Ultrasensitive Diffraction Gratings Based on Smart
672 Hydrogels for Highly Selective and Rapid Detection of Trace Heavy Metal Ions.
673 *J. Mater. Chem. C* **2018**, *6* (42), 11356–11367.
674 https://doi.org/10.1039/c8tc02347f.

(31) Wang, X.; Wang, X.; Liu, X. Hydrogel Diffraction Grating as Sensor: A Tool for Studying Volume Phase Transition of Thermo-Responsive Hydrogel. *Sensors Actuators, B Chem.* **2014**, *204*, 611–616. https://doi.org/10.1016/j.snb.2014.08.013.

(32) Peng, H. Y.; Wang, W.; Gao, F. H.; Lin, S.; Ju, X. J.; Xie, R.; Liu, Z.; Faraj, Y.; Chu, L. Y. Smart Hydrogel Gratings for Sensitive, Facile, and Rapid Detection of Ethanol Concentration. *Ind. Eng. Chem. Res.* **2019**, *58* (38), 17833–17841. https://doi.org/10.1021/acs.iecr.9b03395.

(33) Ye, G.; Yang, C.; Wang, X. Sensing Diffraction Gratings of Antigenresponsive Hydrogel for Human Immunoglobulin-G Detection. *Macromol. Rapid Commun.* **2010**, *31* (15), 1332–1336. https://doi.org/10.1002/marc.201000082.

(34) Zhao, J. J.; Wang, W.; Wang, W.; Wang, F.; Zhao, Y.; Cai, Q. W.; Xie, R.; Xie, R.; Ju, X. J.; Ju, X. J.; et al. Smart Hydrogel Grating Immunosensors for Highly Selective and Sensitive Detection of Human-IgG. *Ind. Eng. Chem. Res.* **2020**, *59* (22), 10469–10475. https://doi.org/10.1021/acs.iecr.0c00780.

(35) https://www.who.int/news-room/fact-sheets/detail/cardiovascular-diseases-(cvds).

(36) Qureshi, A.; Gurbuz, Y.; Niazi, J. H. Biosensors for Cardiac Biomarkers Detection: A Review. *Sensors Actuators, B Chem.* **2012**, *171–172*, 62–76. https://doi.org/10.1016/j.snb.2012.05.077.

(37) Gauer, R. L.; Army, W.; Bragg, F.; Carolina, N. Early Recognition and Management of Sepsis in Adults: The First Six Hours. *Am. Fam. Physician* **2013**, *88*, 44–52.

(38) Salvo, P.; Dini, V.; Kirchhain, A.; Janowska, A.; Oranges, T.; Chiricozzi, A.; Lomonaco, T.; Di Francesco, F.; Romanelli, M. Sensors and Biosensors for C-Reactive Protein, Temperature and PH, and Their Applications for Monitoring Wound Healing: A Review. *Sensors* **2017**, *17* (12), 10–12. https://doi.org/10.3390/s17122952.

(39) Wang, Q.; Jin, H.; Xia, D.; Shao, H.; Peng, K.; Liu, X.; Huang, H.; Zhang, Q.; Guo, J.; Wang, Y.; et al. Biomimetic Polymer-Based Method for Selective Capture of C-Reactive Protein in Biological Fluids. *ACS Appl. Mater. Interfaces* **2018**, *10* (49), 41999–42008. https://doi.org/10.1021/acsami.8b15581.

(40) Iwasaki, Y.; Kimura, T.; Orisaka, M.; Kawasaki, H.; Goda, T.; Yusa, S. I. Label-Free Detection of C-Reactive Protein Using Highly Dispersible Gold Nanoparticles Synthesized by Reducible Biomimetic Block Copolymers. *Chem. Commun.* **2014**, *50* (42), 5656–5658. https://doi.org/10.1039/c4cc01855a.

(41) Matsuura, R.; Tawa, K.; Kitayama, Y.; Takeuchi, T. A Plasmonic Chip-Based Bio/Chemical Hybrid Sensing System for the Highly Sensitive Detection of C-Reactive Protein. *Chem. Commun.* **2016**, *52* (20), 3883–3886. https://doi.org/10.1039/c5cc07868g.

(42) Thompson, D.; Pepys, M. B.; Wood, S. P. The Physiological Structure of Human C-Reactive Protein and Its Complex with Phosphocholine. *Structure* **1999**, *7* (2), 169–177. https://doi.org/10.1016/S0969-2126(99)80023-9.

(43) Díaz-Betancor, Z.; Bañuls, M.-J.; Sanza, F. J.; Casquel, R.; Laguna, M. F.; Holgado, M.; Puchades, R.; Maquieira, Á. Phosphorylcholine-Based Hydrogel for Immobilization of Biomolecules. Application to Fluorometric Microarrays for Use in Hybridization Assays and Immunoassays, and Nanophotonic Biosensing.

722 *Microchim. Acta* **2019**, *186* (570), 1–11. https://doi.org/10.1007/s00604-019-
723 3691-3.

724 (44) https://crm.jrc.ec.europa.eu.

725 (45) Ouchi, I. Anisotropic Absorption and Reflection Spectra of Polyethylene
726 Terephthalate Films in Ultraviolet Region. *Polym. J.* **1983**, *15* (3), 225–243.

727 (46) Mira, D.; Llorente, R.; Morais, S.; Puchades, R.; Maquieira, A.; Marti, J. High-
728 Throughput Screening of Surface-Enhanced Fluorescence on Industrial Standard
729 Digital Recording Media. *Opt. Based Biol. Chem. Sens. Def.* **2004**, *5617*, 364.
730 https://doi.org/10.1117/12.578301.

731 (47) Perez-Hernandez, H.; Lasagni, A. F. Fast and Efficient Manufacturing Method of
732 One- and Two-Dimensional Polyethylene Terephthalate Transmission
733 Diffraction Gratings by Direct Laser Interference Patterning. *Polym. Eng. Sci.*
734 **2012**, *52* (9), 1903–1908. https://doi.org/10.1002/pen.

735 (48) Ye, G.; Wang, X. Polymer Diffraction Gratings on Stimuli-Responsive Hydrogel
736 Surfaces: Soft-Lithographic Fabrication and Optical Sensing Properties. *Sensors*
737 *Actuators, B Chem.* **2010**, *147* (2), 707–713.
738 https://doi.org/10.1016/j.snb.2010.03.052.

739 (49) Otter, D. Protein: Determination and Characterization. In *Encyclopedia of Food*
740 *Sciences and Nutrition*; Elsevier Science Ltd., 2003; Vol. 4824–4830, pp 135–
741 148.

742 (50) Yetisen, A. K.; Butt, H.; Volpatti, L. R.; Pavlichenko, I.; Humar, M.; Kwok, S. J.
743 J.; Koo, H.; Kim, K. S.; Naydenova, I.; Khademhosseini, A.; et al. Photonic
744 Hydrogel Sensors. *Biotechnol. Adv.* **2016**, *34* (3), 250–271.

https://doi.org/10.1016/j.biotechadv.2015.10.005.

(51) Tseng, J.; Mortensen, R. F. Binding of Human C-Reactive Protein (CRP) to Plasma Fibronectin Occurs via the Phosphorylcholine-Binding Site. *Mol. Immunol.* **1988**, *25* (8), 679–686. https://doi.org/10.1016/0161-5890(88)90103-4.

(52) Goray, L. I. Diffraction Grating Groove Metrology Using AFM & STM. In *Recent Developments in Atomic Force Microscopy and Raman Spectroscopy for Materials Characterization*; IntechOpen, 2021. https://doi.org/10.5772/intechopen.97257.

(53) Hutchinson, W. L.; Koenig, W.; Fröhlich, M.; Sund, M.; Lowe, G. D. O.; Pepys, M. B. Immunoradiometric Assay of Circulating C-Reactive Protein: Age-Related Values in the Adult General Population. *Clin. Chem.* **2000**, *46* (7), 934–938. https://doi.org/10.1093/clinchem/46.7.934.

(54) Cozlea, D. L.; Farcas, D. M.; Nagy, A.; Keresztesi, A. A.; Tifrea, R.; Cozlea, L.; Carașca, E. The Impact of C Reactive Protein on Global Cardiovascular Risk on Patients with Coronary Artery Disease. *Curr. Heal. Sci. J.* **2013**, *39* (4), 225–231.

(55) Póvoa, P.; Almeida, E.; Moreira, P.; Fernandes, A.; Mealha, R.; Aragão, A.; Sabino, H. C-Reactive Protein as an Indicator of Sepsis. *Intensive Care Med.* **1998**, *24* (10), 1052–1056. https://doi.org/10.1007/s001340050715.